

## Damped fall of magnets inside a conducting pipe

Guillermo Donoso, Celso L. Ladera, and Pablo Martín

Citation: *Am. J. Phys.* **79**, 193 (2011); doi: 10.1119/1.3531964

View online: <http://dx.doi.org/10.1119/1.3531964>

View Table of Contents: <http://ajp.aapt.org/resource/1/AJPIAS/v79/i2>

Published by the [American Association of Physics Teachers](#)

### Related Articles

Pulse Oximetry in the Physics Lab: A Colorful Alternative to Traditional Optics Curricula  
*Phys. Teach.* **51**, 495 (2013)

Little Green Man Physics  
*Phys. Teach.* **51**, 427 (2013)

A Progression of Static Equilibrium Laboratory Exercises  
*Phys. Teach.* **51**, 430 (2013)

Color reproduction with a smartphone  
*Phys. Teach.* **51**, 440 (2013)

Computer Supported Collaborative Rocketry: Teaching students to distinguish good and bad data like expert physicists  
*Phys. Teach.* **51**, 424 (2013)

### Additional information on Am. J. Phys.

Journal Homepage: <http://ajp.aapt.org/>

Journal Information: [http://ajp.aapt.org/about/about\\_the\\_journal](http://ajp.aapt.org/about/about_the_journal)

Top downloads: [http://ajp.aapt.org/most\\_downloaded](http://ajp.aapt.org/most_downloaded)

Information for Authors: <http://ajp.dickinson.edu/Contributors/contGenInfo.html>

**Winter  
Meeting  
January 4-7**



# Damped fall of magnets inside a conducting pipe

Guillermo Donoso, Celso L. Ladera,<sup>a)</sup> and Pablo Martín<sup>b)</sup>

*Departamento de Física, Universidad Simón Bolívar, Apdo. 89000, Caracas 1086, Venezuela*

(Received 10 November 2009; accepted 23 September 2010)

We consider the uniform motion of a short strong cylindrical magnet falling inside a conducting pipe and study the dependence of the magnetic braking force on the distance of the falling magnet from the pipe wall. We also consider two magnets falling together with parallel or opposite magnetic moments. We develop models for these three cases of magnetic braking and describe the experiments that validate our models. The experimental setups are inexpensive and can be readily assembled in a teaching laboratory. © 2011 American Association of Physics Teachers.

[DOI: 10.1119/1.3531964]

## I. INTRODUCTION

A single magnet falling without acceleration inside a vertical conducting pipe is frequently presented in lectures, demonstrations, science exhibits, and in literature.<sup>1-4</sup> Magnetic braking has also been studied in the context of a conducting disk rotating between the poles of a magnet.<sup>5-7</sup> The fall of a strong magnet inside a conducting pipe is damped by the gradually increasing and opposing magnetic force that the pipe wall exerts on the magnet. If the pipe is long enough, the magnet eventually reaches a constant terminal speed. The braking force on the magnet arises from circular eddy currents, also known as Foucault currents. These eddy currents are generated in the pipe by the emf induced in the pipe by the time-varying magnetic flux that the falling magnet produces.

When the phenomenon is demonstrated, many questions are often posed by students and physicists: What would happen if two magnets are allowed to fall together inside the pipe? Will these magnets fall faster than a single one? What is the role of the pipe wall thickness? What effect does changing the material of which the pipe is made? These issues have been addressed by us in a recent article.<sup>1</sup>

Another common question is what would happen if the magnet falls off-axis. We explore, both analytically and experimentally, the off-axis case and the two-magnet case. Because the initial accelerated motion of the falling magnets lasts for only a very short time, we consider only the final uniform motion of the magnets. We find the falling time of the magnets inside a vertical conducting pipe of known inner radius  $a$  in terms of a single parameter. For near-wall descent, this parameter is the distance  $b$  from the falling magnet axis to the pipe axis, and for two magnets, the parameter is the vertical separation  $s$  of the two magnets. We hope that the models and the set of experiments that we discuss are useful for lecturers and demonstrators, and serve as an inspiration for practical applications.<sup>8</sup>

Magnetic damping is being increasingly exploited in a diversity of important applications including advanced car suspension systems that use a colloidal suspension<sup>9,10</sup> of ferromagnetic particles in oil, as shock-absorber fluid when

subjected to a magnetic field, and some more mundane applications such as fishing-reel spool rotation control (with at least two patents already filed), and the smooth braking of a gondola full of people in an amusement park after a free fall. The damping of the motion of a metallic body by magnetic means can also be achieved by the retarding force on the Foucault (eddy) currents induced in the body by a constant local magnetic field normal to the body surface.<sup>11-15</sup>

## II. TWO MAGNETS

### A. Theory

Consider two identical short cylindrical magnets separated by a fixed distance  $s$ , which fall together along a conducting pipe. Will they fall faster than a single magnet? What happens if the magnet separation is changed? What happens if the orientation of the magnet poles is changed?

Before addressing the fall of the two magnets, we first briefly consider the fall of a single magnet inside a conducting pipe.<sup>1</sup> A short cylindrical and strong magnet (for example, a Nd:FeB magnet) falls with velocity  $\mathbf{v}=v\hat{\mathbf{z}}$  inside a copper pipe of inner radius  $a$  (see Fig. 1) such that the magnet axis of symmetry is always coincident with the vertical pipe symmetry. As the magnet falls, the changing magnetic flux  $\Phi_B(t)$  generates an induced emf  $\mathcal{E}$  in the pipe wall. This emf can be obtained using Faraday's law,<sup>11,16-18</sup>

$$\mathcal{E} = -\frac{d\Phi_B}{dt} = -\frac{d}{dt} \int \mathbf{B} \cdot d\mathbf{S}, \quad (1)$$

which for a motional induced emf gives<sup>1</sup> the relation [see Ref. 16, Eq. (7.17), or Ref. 17, Eq. (6.5)],

$$\mathcal{E} = \int \mathbf{v} \times \mathbf{B}_\rho \cdot d\boldsymbol{\ell} = \int_0^{2\pi} v B_\rho(a, z) a d\theta = 2\pi a v B_\rho(a, z), \quad (2)$$

where  $B_\rho(a, z)$  is the magnitude of the radial component of the magnetic field at the pipe wall. Let  $\sigma$  be the conductivity of the pipe wall. If  $R$  denotes electrical resistance and  $\tau$  is the pipe thickness, then the conductance of a ring (of height  $dz$  defined on the pipe wall at coordinate  $z$ , as shown in Fig. 1) is by the definition  $\tau\sigma dz/(2\pi a)$ . The induced electrical current  $dI$  present in the ring is therefore given by

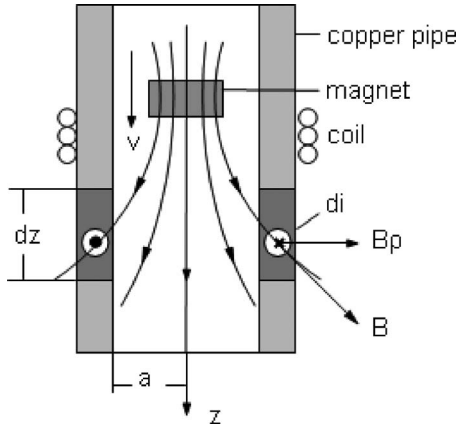


Fig. 1. A magnet falls with velocity  $v$  along the symmetry axis of a conducting pipe. An infinitesimal current  $dI$  is generated by Faraday induction in an infinitesimal pipe ring of height  $dz$  at a distance  $z$  below the magnet.  $B_\rho$  is the radial component of the magnetic induction  $\mathbf{B}$  of the magnet.

$$dI = \mathcal{E}d(1/R) = \frac{\mathcal{E}\sigma\tau dz}{2\pi a} \quad (3a)$$

$$= 2\pi av B_\rho(a, z) \frac{\sigma\tau dz}{2\pi a} = v\sigma\tau B_\rho(a, z) dz. \quad (3b)$$

The magnitude  $dF$  of the vertical force that the differential ring exerts on the falling magnet is<sup>1-5</sup>

$$\begin{aligned} dF &= dI \int (\mathbf{dl} \times \mathbf{B})_z = 2\pi a B_\rho(a, z) dI \\ &= 2\pi av \sigma\tau B_\rho^2(a, z) dz. \end{aligned} \quad (4)$$

The total force applied by the pipe to the magnet can be obtained by integrating along the whole pipe, that is,

$$F = 2\pi av \sigma\tau \int_{-\infty}^{\infty} B_\rho^2(a, z) dz. \quad (5)$$

It is convenient to represent the radial component  $B_\rho$  of the magnetic field using a useful approximation discussed in Ref. 19. For  $\rho = a$ , we have

$$B_\rho(a, z) = \frac{3\tilde{\mu}\alpha z a}{[a^2 + (\alpha z)^2]^{5/2}}, \quad (6)$$

where  $\tilde{\mu} = (\mu_0/4\pi)\mu$ , and  $\mu$  represents the magnetic dipole<sup>11,16-18</sup> of the magnet in SI units. The introduction of  $\tilde{\mu}$  simplifies the expressions that follow. The parameter  $\alpha$  corrects for the failure of the simple magnetic dipole approximation when representing the actual magnetic field of the cylindrical magnet.<sup>1,18</sup> The quantity  $\tilde{\mu}$  and the parameter  $\alpha$  are determined in a preliminary experiment, as explained in the Appendix (in our case,  $\alpha = 1.25 \pm 0.05$  and  $\tilde{\mu} = 4.8 \times 10^{-8} \text{ T m}^3$ ). Once the values of  $\alpha$  and  $\tilde{\mu}$  are found for a given magnet, these values are used in whatever experiments are performed with that magnet.

In terms of the dimensionless axial variable  $u = \alpha z/a$ , Eq. (6) becomes

$$B_\rho(u) = \frac{3\tilde{\mu}}{a^3} \frac{u}{(1+u^2)^{5/2}}. \quad (7)$$

We substitute this result into Eq. (5) and obtain the desired expression for the magnetic force on the falling magnet,

$$F = \frac{2\pi a^2 v \sigma\tau}{\alpha} 2 \left( \frac{3\tilde{\mu}}{a^3} \right)^2 \int_0^\infty \frac{u^2 du}{(1+u^2)^5} \quad (8a)$$

$$= \frac{36\pi v \sigma\tau \tilde{\mu}^2}{\alpha a^4} f_0, \quad (8b)$$

where the factor of  $\alpha$  comes from substituting  $dz = a du/\alpha$  into Eq. (5). The constant force factor  $f_0$  is the value of the definite integral,

$$f_0 = \int_0^\infty \frac{u^2 du}{(1+u^2)^5} = \frac{5\pi}{256} \approx 0.0614. \quad (9)$$

Equation (8) shows that the magnetic force  $F$  opposing the motion of the falling magnet is proportional to the vertical speed  $v$  of the magnet. We can use Eq. (8) to define a damping constant  $k = F/v$  for the magnet motion

$$k \equiv \frac{36\pi\sigma\tau\tilde{\mu}^2}{\alpha a^4} f_0. \quad (10)$$

The terminal speed  $v_t$  can be obtained by applying Newton's second law with the result  $v_t = mg/k$ .

To obtain an idea of the order of magnitude of the terminal speed for a short strong cylindrical ceramic magnet falling along the symmetry axis of a conducting pipe, we consider the typical experimental parameters,  $\tilde{\mu} = 4.8 \times 10^{-8} \text{ T m}^3$ ,  $\alpha = 1.25 \pm 0.05$ ,  $\sigma = 4.8 \times 10^7 (\Omega \text{ m})^{-1}$ ,  $a = 10.4 \text{ mm}$ ,  $\tau = 1.3 \text{ mm}$ , and  $m = 7.0 \text{ g}$ . The theory predicts  $k = 0.068 \text{ N s/m}$  and  $v_t = 1.02 \text{ m/s}$ , which are close to the experimental values we will find.

We now consider two short identical cylindrical magnets falling together inside the conducting pipe along its axis. The vertical separation between them is  $s$ . We first assume that their magnetic moments are parallel. By simple superposition of the magnetic fields created by the two magnets, we readily obtain from Eq. (6),

$$B_\rho(a, z) = \frac{3\tilde{\mu}\alpha\alpha(z-s/2)}{[a^2 + \alpha^2(z-s/2)^2]^{5/2}} + \frac{3\tilde{\mu}\alpha\alpha(z+s/2)}{[a^2 + \alpha^2(z+s/2)^2]^{5/2}}, \quad (11)$$

and with the change of variables  $u = \alpha z/a$ ,

$$B_\rho(a, u) = \frac{3\tilde{\mu}}{a^3} \left[ \frac{u - \frac{\alpha s}{2a}}{\left[1 + \left(u - \frac{\alpha s}{2a}\right)^2\right]^{5/2}} + \frac{u + \frac{\alpha s}{2a}}{\left[1 + \left(u + \frac{\alpha s}{2a}\right)^2\right]^{5/2}} \right]. \quad (12)$$

We now proceed along the same lines as from Eq. (8) to Eq. (10) to obtain the force factor  $f_{\uparrow\uparrow}(s/a)$  for the two-magnet case, which is conveniently written as a function of the magnets' separation  $s/a$  as

$$f_{\uparrow\uparrow}(s/a) = \int_0^\infty \left[ \frac{u - \frac{\alpha s}{2a}}{\left[ 1 + \left( u - \frac{\alpha s}{2a} \right)^2 \right]^{5/2}} + \frac{u + \frac{\alpha s}{2a}}{\left[ 1 + \left( u + \frac{\alpha s}{2a} \right)^2 \right]^{5/2}} \right]^2 du. \quad (13)$$

We also obtain an expression for the magnetic braking force  $F = kv$  on the two-magnet assembly in terms of  $f_{\uparrow\uparrow}(s/a)$ ,

$$F = \frac{36\pi\sigma\tau v \tilde{\mu}^2}{\alpha a^4} f_{\uparrow\uparrow}(s/a). \quad (14)$$

Equation (14) for two magnets is analogous to Eq. (8) for a single magnet;  $f_{\uparrow\uparrow}(s/a)$  corresponds to  $f_0$ .

As Eq. (14) shows, the magnetic braking force is quadratic in the radial component of the magnetic field at the pipe wall, and therefore doubling the field implies multiplying the force by 4. Therefore, for  $s=0$ , that is, for zero separation between the magnets, Eq. (13) reduces to  $f_{\uparrow\uparrow}(0) = 4f_0$  [the constant  $f_0$  is found using Eq. (9)]. For magnets separated by a large distance,  $s \gg a$ , Eq. (13) gives a constant force factor  $f_{\uparrow\uparrow} = 2f_0$ . For  $s/a > 0.7$ , we obtain  $f_{\uparrow\uparrow} < 2f_0$ . To understand this result, note that when the two magnets are separated by a nonzero distance  $s$ , the radial magnetic components of the two fields at the pipe walls partially cancel each other; at  $s=0$ , they add to become twice that for a single magnet.

Figure 4 shows the predicted dimensionless force factor  $f_{\uparrow\uparrow}(s/a)/2f_0$  from Eqs. (9) and (13) plotted against the parameter  $s/a$ . We see that a minimum value of the force factor is predicted for  $s/a \approx 1.2$ . Also note that  $f_{\uparrow\uparrow}(s/a)/2f_0 \rightarrow 1$  for  $s/a$  greater than about 3.5. We will see below the experiments confirm our predictions.

## B. Experiments

We present here the results of measuring the terminal speed  $v_t$  of a system of two identical magnets of mass  $m$  falling inside a copper pipe of radius  $a$  under gravitational attraction and the braking magnetic force  $-kv$ . The terminal speed  $v_t$  for the two-magnet assembly is

$$v_t = 2mg/k. \quad (15)$$

Because the damping constant  $k = F/v$  is a function of the force factor  $f_{\uparrow\uparrow}(s/a)$ , we can check our model by measuring the terminal speed of the two-magnet system as the separation  $s$  between the magnets is changed.

We can measure the terminal speed  $v_t = \Delta z / \Delta t$  of a falling magnet by observing the two transients electrical signals that the magnet generates in an oscilloscope when crossing two short pick-up coil made of thin wire and tightly wrapped onto the pipe at two locations separated by a small distance  $\Delta z$ .<sup>1-3</sup> Here,  $\Delta t$  is the time interval between the zero crossings of the two time signals. The coils are located far enough from the top of the pipe to ensure that the terminal speed has been reached. We substitute  $k = F/v$  in Eq. (15) and obtain the falling time interval  $\Delta t$ ,

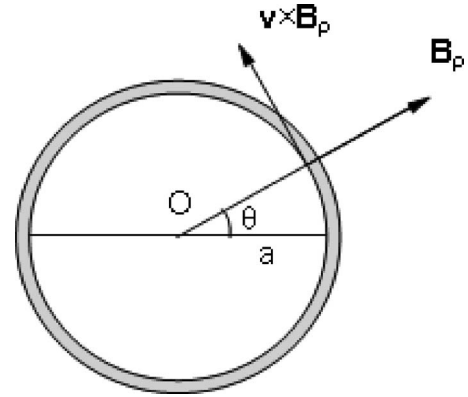


Fig. 2. Horizontal cross section of a conducting pipe of internal radius  $a$ . A magnet that falls with velocity  $v$  along the pipe symmetry axis, perpendicular to the cross section at  $O$ , generates a radial magnetic field component  $B_p$ . The cross product  $v \times B_p$  is tangent to the pipe wall, and its line integral along the circular wall gives the Faraday induced emf.

$$\Delta t = \frac{\Delta z}{v_t} = \frac{k \Delta z}{2mg} = \frac{36\pi\sigma\tau \tilde{\mu}^2 \Delta z}{2\alpha mg a^4} f_{\uparrow\uparrow}(s/a), \quad (16)$$

which is the prediction to be experimentally checked.

### 1. Two magnets with parallel magnetic moments

Two 12.7 mm diameter, 3.15 mm thick, Nd:FeB cylindrical magnets, 3 g each, are vertically assembled at a given fixed separation by placing identical 5 mm thick ceramic disks in between (Fig. 3). The values of  $\tilde{\mu} = 4.8 \times 10^{-8} \text{ T m}^3$  and  $\alpha = 1.25 \pm 0.05$  were found in a preliminary experiment (see the Appendix). As noted, extra ceramic disks are placed atop the two-magnet assembly up to a total number of 8 disks for a total mass of 8 g. The assembly of magnets plus ceramic disks with total mass of 14.0 g is held together by tightly wrapping it with thin sticky tape. The mass of the ceramic disks need not be considered in our calculations because the number of disks is the same in all the experiments (it is as though the mass of the two magnets were the total mass of the magnet-ceramics assembly).

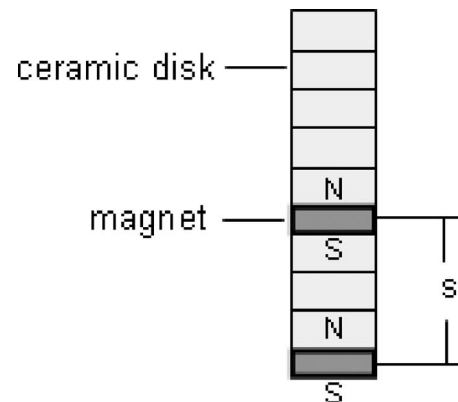


Fig. 3. Two identical short cylindrical magnets (dark gray) are assembled at a fixed separation  $s$  by inserting identical 5 mm thick ceramic disks between them. Extra ceramic disks are placed at the top of the assembly to keep the total weight of the assembly constant, while the magnet separation is varied. For example, to increase the magnet separation by 5 mm, we remove a disk from the top and insert it between the magnets. The magnetic moments of the magnets are parallel.



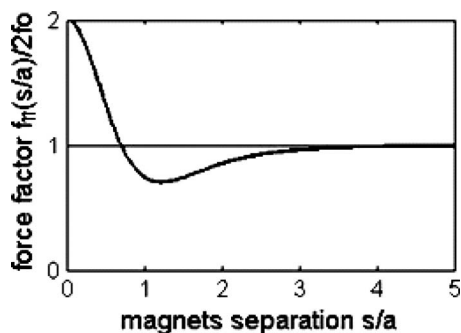


Fig. 4. The predicted dimensionless force factor  $f_{\uparrow\uparrow}(s/a)/2f_0$  (with parallel magnetic moments) as a function of the two-magnet separation. Note that the absolute minimum of the magnetic force occurs for the magnet separation  $s/a=1.2$ .

The magnet assembly is allowed to fall inside a copper pipe of radius  $a=10.4$  mm and wall thickness of 1.3 mm. The conductivity  $\sigma$  of the stock copper pipes was measured by measuring the length and cross-sectional area of the pipe using a current source of several tens of amperes and a digital voltmeter to obtain the electrical resistance of the pipe. We find  $\sigma=4.8 \times 10^7$  ( $\Omega \text{ m}$ )<sup>-1</sup> (82% of the conductivity of pure copper).

The pick-up coils used in the magnetic braking experiments, made of AWG-38 copper wire, are wound onto the pipe at previously chosen locations along it. A digital oscilloscope is used to display and store the transient signals generated in the coils by the falling magnets for later analysis.

Figure 5 shows our results, where the continuous line represents either the force factor  $f_{\uparrow\uparrow}(s/a)$  or the predicted fall interval times  $\Delta t$  of the two magnets [see Eq. (16)] versus the parameter  $s/a$ . The actual experimental data points are also

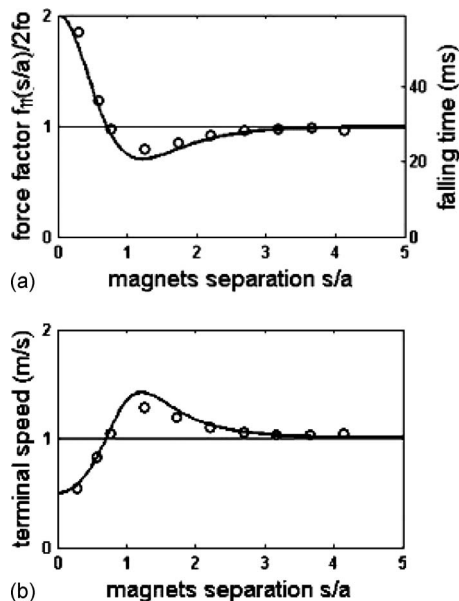


Fig. 5. (a) The force factor and the magnets fall time as a function of the vertical separation  $s/a$  between the two magnets (with parallel magnetic moments). The first experimental point (for  $s=3$  mm) corresponds to the two magnets in contact; the second one corresponds to a separation of 6 mm (a paper disk is inserted between the magnets). (b) The terminal speed of the two magnets as a function of  $s/a$ .

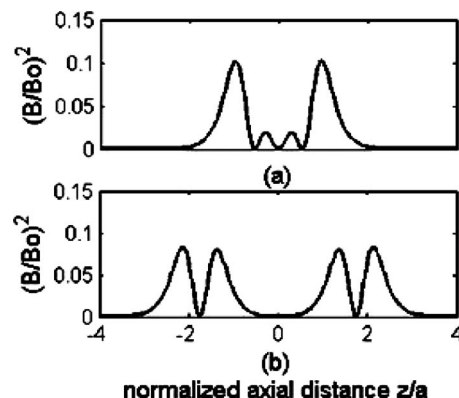


Fig. 6. Dimensionless squared magnetic field as a function of the normalized axial distance  $z/a$  ( $B_0=3\tilde{\mu}/a^3$  is a constant). (a)  $s=1.2a$  and (b)  $s=3.5a$ . The area under the curves represents the total damping force on the magnets. The force in (a) is smaller than the force in (b).

plotted in Fig. 5. The maximum error is about 0.3 ms (0.8%) for a magnet separation  $s=6$  mm. Figure 5 shows that when  $s$  is large, the two-magnet system falls with the same terminal speed as that of a single magnet falling inside the same pipe ( $v_t \approx 1$  m/s). For intermediate values of  $s$ , namely,  $0.7 < s/a < 3.5$ , the falling times are smaller, meaning that the magnetic braking force is smaller, and the two magnets fall faster than a single magnet. This result is a consequence of the partial cancellation of the two radial components of the two magnetic fields in the region between the two magnets. Therefore, for  $s=0$ , we expect to observe a falling time interval that is twice that for a single magnet, as the plot in Fig. 5(a) shows. Also note in Fig. 5(a) that the experiments confirm the predicted absolute minimum (of the continuous line) of the magnetic braking force for  $s/a \approx 1.2$ . The experimental points in Fig. 5(a) are plotted without error bars because the largest error is 0.3 ms for  $s=6$  mm, less than or equal to the radius of the circles that represent the experimental data. Each point is the result of multiple trials. Figure 5(b) shows the terminal speed of the two magnets as a function of  $s/a$ . There is a maximum speed for  $s \approx 1.2a$ , which coincides with the position of the minimum damping force.

We can give an alternative explanation of the existence of the minimum of the magnetic force on the falling magnets when their vertical separation is  $s=1.2a$ . The two curves in Fig. 6 show the quantity  $(B_{\rho,1}+B_{\rho,2})^2$  of the two radial field components generated by the magnets as a function of  $z/a$ . The magnetic field has been normalized by the quantity  $B_0=3\tilde{\mu}/a^3$ . According to Eq. (13), the magnetic braking force is proportional to the integral of the squared radial component of the magnetic field, and therefore the area under each of the curves in Fig. 6 represents the total magnetic force on the two magnets. The area under the upper curve is about half of the area under the lower curve. The difference in area below the two curves arises from the partial cancellation of the fields of the two magnets in the region between them.

## 2. Two magnets falling with antiparallel magnetic moments

We also consider the two-magnet system with antiparallel magnetic moments. We need only to change the middle sign

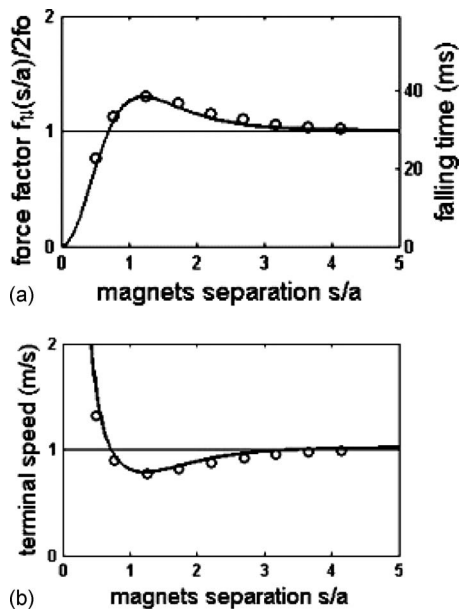


Fig. 7. (a) Normalized force factor  $f_{\uparrow\downarrow}(s/a)/2f_0$  or fall time intervals for two equal magnets falling inside a conducting pipe as a function of  $s/a$ . (b) The terminal speed of the two magnets as a function of  $s/a$ . The minimum speed occurs for  $s \approx 1.2a$  in coincidence with the position of the maximum damping force. The small circles represent experimental data. The error bars are smaller than the size of the circles used to plot the data.

of the integrand of Eq. (13), which gives the force factor function  $f_{\uparrow\downarrow}(s/a)$  for the two-magnet assembly. The result is

$$f_{\uparrow\downarrow}(s/a) = \int_0^\infty \left[ \frac{u - \frac{\alpha s}{2a}}{\left[ 1 + \left( u - \frac{\alpha s}{2a} \right)^2 \right]^{5/2}} - \frac{u + \frac{\alpha s}{2a}}{\left[ 1 + \left( u + \frac{\alpha s}{2a} \right)^2 \right]^{5/2}} \right] du. \quad (17)$$

The continuous line in Fig. 7 shows the force factor function  $f_{\uparrow\downarrow}(s/a)/2f_0$  in Eq. (17) as a function of  $s/a$ . The measured fall time interval is also plotted in Fig. 7 (small circles). Because the fall times are proportional to the force factor function [see Eq. (16)], the continuous line also represents the predicted falling times. As shown in Fig. 7, the agreement between the experimental results and the theory is good. Figure 7(b) shows the terminal speed of the two magnets. There is a minimum terminal speed for  $s \approx 1.2a$ , which corresponds to the maximum of the magnetic force as  $s$  is varied.

### III. OFF-AXIS FALL OF SINGLE MAGNET

#### A. Theory

The vertical motion of a magnet inside a conducting pipe is damped by the opposing force that the pipe wall exerts on the magnet. It is usually assumed that a cylindrical magnet

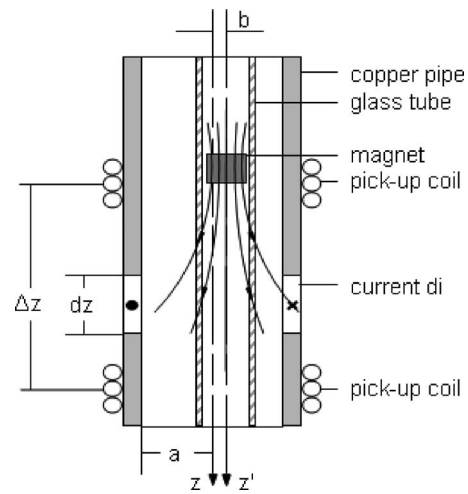


Fig. 8. Longitudinal cross section of the pipe of radius  $a$  and of a vertical glass tube used to keep the magnet off-axis. The separation of the magnet path from the vertical pipe axis is  $b$ . The falling magnet induces a current  $dl$  at the infinitesimal ring of height  $dz$ . Two pick-up coils separated by the vertical distance  $\Delta z$  are used for measuring the magnet speed.

falls with its symmetry axis always coincident with the pipe axis. Such a situation seldom happens, and the magnet can fall off-axis, or even wobble along the pipe.

Figure 8 depicts a short cylindrical magnet falling with velocity  $v$  along the  $z$  direction a distance  $b$  from the vertical symmetry  $z$ -axis of the pipe of internal radius  $a$ . (The magnet actually falls inside a guiding glass tube placed inside the pipe.) Consider a ring-shaped differential element of height  $dz$  of the pipe below the magnet. This infinitesimal conducting ring is approached by the falling magnet, which induces an emf in it. The magnetic field can be decomposed into a component parallel to the pipe axis, and a radial component  $\mathbf{B}_\rho$  along the radial direction from the center  $O'$  of the glass tube (see Fig. 9). As explained in Sec. II [see Eq. (2)], only the radial component  $\mathbf{B}_\rho$  of the magnetic field is responsible for the induced emf in the conducting ring.

Let  $P(a, \theta)$  be a point of the infinitesimal ring as seen from the center  $O$  of the ring (see Fig. 9), and let  $\rho$  be the polar radius of  $P$  as seen from point  $O'$  on the  $z'$ -axis. For an

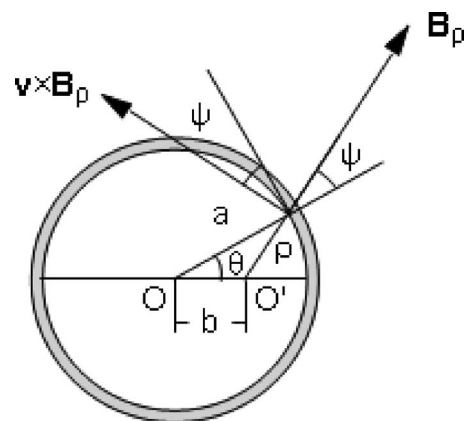


Fig. 9. Horizontal cross section of the conducting pipe when the magnet is off-axis. The path of the magnet is the vertical through point  $O'$  at the distance  $b$  from point  $O$  located on the pipe axis. The angle between the cross product  $\mathbf{v} \times \mathbf{B}_\rho$  and the tangent to the pipe is  $\psi$  (see Fig. 2).

off-axis fall, the radial component  $\mathbf{B}_\rho$  of the field forms a variable angle  $\psi(\rho, b)$  with the radius vector OP from the center of the infinitesimal ring (compare with Fig. 2 where the component  $\mathbf{B}_\rho$  always points along the radial direction from O). The cross product  $\mathbf{v} \times \mathbf{B}_\rho$  is no longer tangential to the pipe wall.

The magnitude  $B_\rho$  of the radial component is a function of the distance  $\rho$  and the vertical coordinate  $z$  of the infinitesimal ring. The motional induced emf on the eccentric infinitesimal conducting ring is given, as in Sec. II, by

$$\mathcal{E} = \int \mathbf{v} \times \mathbf{B}_\rho \cdot d\boldsymbol{\ell} = \int_0^{2\pi} v B_\rho(a, z) \cos \psi(\rho, b) a d\theta. \quad (18)$$

From the geometry of Fig. 9, we may write

$$\cos \psi = \frac{a - b \cos \theta}{\rho} \quad (19)$$

and

$$\rho^2 = a^2 + b^2 - 2ab \cos \theta. \quad (20)$$

We use the same approximation for the magnetic field given in Eq. (6), the radial component of the magnetic field for the off-axis case is

$$B_\rho(a, z) = \frac{3\tilde{\mu}\alpha z \rho}{[\rho^2 + (\alpha z)^2]^{5/2}}. \quad (21)$$

With Eq. (21) for the component  $B_\rho$ , the induced emf becomes

$$\mathcal{E} = \int_0^{2\pi} v \frac{3\tilde{\mu}\alpha z \rho}{[a^2 + b^2 - 2ab \cos \theta + \alpha z^2]^{5/2}} \frac{a - b \cos \theta}{\rho} a d\theta. \quad (22)$$

We introduce the dimensionless variable  $u$  as  $z = au/\alpha$  and rewrite Eq. (22) as

$$\begin{aligned} \mathcal{E} &= \frac{6\pi\tilde{\mu}v}{a^2} \int_0^{2\pi} \frac{u[1 - (b/a)\cos \theta]}{2\pi \left[ 1 + \left(\frac{b}{a}\right)^2 - 2\left(\frac{b}{a}\right)\cos \theta + u^2 \right]^{5/2}} d\theta \\ &= \frac{6\pi\tilde{\mu}v}{a^2} G(u, b), \end{aligned} \quad (23)$$

where

$$G(u, b) = \int_0^{2\pi} \frac{u[1 - (b/a)\cos \theta]}{2\pi \left[ 1 + \left(\frac{b}{a}\right)^2 - 2\left(\frac{b}{a}\right)\cos \theta + u^2 \right]^{5/2}} d\theta. \quad (24)$$

The expression for  $\mathcal{E}$  given by the right-hand side of Eq. (23) reduces to the expression found in Eqs. (2) and (7) for the induced emf when the magnet is assumed to fall along the pipe axis, that is, when  $b=0$ . The definite integral in Eq. (24) is best evaluated using numerical routines available in several software packages.

We can now derive an expression for the vertical component  $dF_z$  of the magnetic braking force that the differential ring (Fig. 8) defined in the pipe wall exerts on the magnet when it falls off-axis. This force component is now given by

$$dF_z = dI(ad\theta)B_\rho(\rho, z)\cos \psi. \quad (25)$$

We also know that the differential  $dI$  of the induced electric current along the infinitesimal ring of height  $dz$  is

$$dI = \mathcal{E}d(1/R) = \frac{\mathcal{E}\sigma\tau dz}{2\pi a} = \frac{\mathcal{E}\sigma\tau a du}{2\pi\alpha a}. \quad (26)$$

We substitute this result into Eq. (25) and integrate along the ring from  $\theta=0$  to  $\theta=2\pi$  and obtain

$$dF_z = \frac{\sigma\tau v du}{2\pi} \left[ \int_0^{2\pi} B_\rho(\rho, u) \cos(\rho, b) a d\theta \right]^2 \quad (27a)$$

$$= \frac{\sigma\tau v du}{2\pi\alpha} \left( \frac{6\tilde{\mu}\pi}{a^2} \right)^2 [G(u, b)]^2, \quad (27b)$$

where  $G(u, b)$  was defined in Eq. (24). Finally, by integrating along the whole pipe, we obtain the expression for the total magnetic braking force on the off-axis falling magnet,

$$F_z = \frac{36\pi\sigma\tau v \tilde{\mu}^2}{\alpha a^4} \int_0^\infty [G(u, b)]^2 du \equiv \frac{36\pi\sigma\tau v \tilde{\mu}^2}{\alpha a^4} \tilde{f}(b/a), \quad (28)$$

which reduces to Eq. (8) for  $b=0$ . Note that in Eq. (28) we have introduced the new force factor  $\tilde{f}(b/a)$  corresponding to off-axis fall.

We use Eq. (28) and obtain an expression for the falling time interval  $\Delta t$  for the magnet to travel a vertical distance  $\Delta z$ ,

$$\Delta t = \frac{k\Delta z}{mg} = \frac{36\pi\sigma\tau v \tilde{\mu}^2 \Delta z}{\alpha m g a^4} \tilde{f}(b/a). \quad (29)$$

By fixing a distance  $\Delta z$  between the two pick-up coils (Fig. 8) and measuring the falling interval times  $\Delta t$  for different values of the separation  $b$ , we can obtain the experimental values of the factor  $\tilde{f}(b/a)$  defined in Eq. (28).

## B. Experiments (off-axis fall)

A different copper pipe is used in this third set of experiments to leave room for large off-axis displacements. Its specifications are 12.4 mm internal radius, 1.7 mm thick wall, and 50 cm length. A 14.2 mm internal diameter glass tube with a 1 mm thick glass wall is placed inside the larger diameter copper pipe. This glass tube is used to keep the path of the falling magnet at a fixed distance from the axis of symmetry of the pipe. The axis of the glass tube is held parallel to the pipe axis at the separation  $b$  (the maximum possible separation is 4.3 mm). As before, two pick-up coils separated by 30 mm are used to sense the passing falling magnet (in our experiments the terminal speed of the magnets is reached about 30 cm from the top of the tubes). The terminal speed is found by dividing the coil separation by the time interval between the two transient signals observed in the oscilloscope.

Figure 10 shows the experimental results for the off-axis fall case, superimposed on the theoretical curve from Eq. (28). The agreement between the theory and the experiment is good (maximum error of 3% for  $b=4.3$  mm). Figure 10(a) also shows  $\tilde{f}(b/a)$  as a function of the normalized separation of the falling magnet from the pipe axis. As expected, the

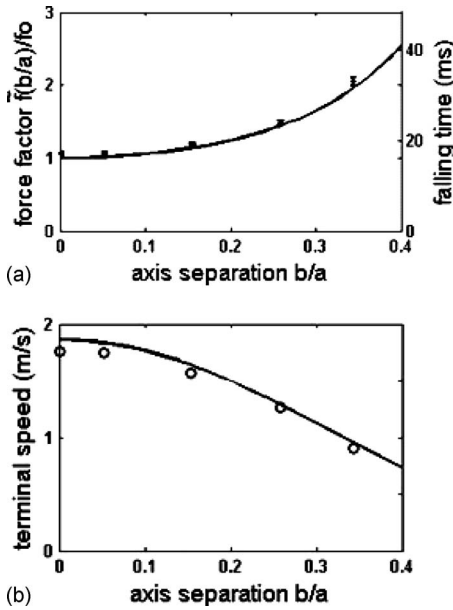


Fig. 10. (a) Plot of the magnetic damping force and the fall interval time as represented by  $\tilde{f}(b/a)/f_0$  as a function of  $b/a$ . The experimental points closely match the theoretical curve. (b) Plot of the terminal speed versus  $b/a$ . The continuous line is the predicted terminal speed and the experimental points closely follow that line.

magnetic braking force increases monotonically as the magnet axis is placed closer to the conducting pipe wall. Figure 10(b) shows the terminal speed of the magnet as a function of  $b/a$ . The terminal speed decreases monotonically as the magnet axis is placed closer to the pipe wall, a consequence of larger induced Foucault (eddy) currents in the conducting wall, which produce a larger magnetic braking force.

#### IV. MEASURING THE FOUCAULT CURRENTS IN THE PIPE WALL

One of the bonuses of our model and experiments is the actual value of the Foucault current that a single falling magnet induces in the pipe wall. The calculation of this current is seldom addressed in literature. The currents induced by the falling magnet are not localized, but are distributed along the whole pipe. Nonetheless, the value of the current ahead of the magnet can be estimated by using Eqs. (3), (6), and (7) to write  $dI$  as

$$dI = v\sigma\tau B_\rho(a, z) dz = v\sigma\tau \frac{3\tilde{\mu}\alpha za}{[a^2 + (\alpha z)^2]^{5/2}} \quad (30a)$$

$$= \frac{3v\sigma\tau\tilde{\mu}}{\alpha a^2} \frac{u}{(1+u^2)^{5/2}} du, \quad (30b)$$

which gives

$$I = \frac{v\sigma\tau\tilde{\mu}}{\alpha a^2} \int_0^\infty \frac{3u}{(1+u^2)^{5/2}} du = \frac{v\sigma\tau\tilde{\mu}}{\alpha a^2}. \quad (31)$$

Equation (31) gives for typical values of  $v$ ,  $\sigma$ ,  $\alpha$ ,  $a$ , and  $\tau$ , the value  $I = 22.2$  A. The large value of  $I$  is explained by the low resistance  $R$  of the conducting pipe ( $R \approx 1 \times 10^{-4}$   $\Omega$ ).

#### ACKNOWLEDGMENTS

The authors are very grateful to Professor Ramón Mata-Toledo of Madison University in Virginia for kindly providing the strong magnets used in the experiments reported in this work and for his encouragement. The authors would also like to acknowledge the reviewers for their useful comments and Professor G. Aubrecht of the Physics Department of Ohio State University for kindly revising the English.

#### APPENDIX: MEASUREMENT OF THE QUANTITY $\tilde{\mu}$ AND THE PARAMETER $\alpha$

In Sec. II, the quantities  $\tilde{\mu}$  and  $\alpha$  were introduced in our model of the magnet's field.<sup>1</sup> These two quantities can be readily found by performing a simple experiment in which the transient emf,  $\mathcal{E}(t)$ , induced in two pick-up coils by the falling magnet is displayed and stored in a digital oscilloscope. The thin wire coils of  $N$  turns (30–40), separated by a distance  $\Delta z$ , are wound onto the same copper pipe used in the experiments of Sec. II (or if preferred onto a short cardboard cylinder of radius  $a$ ), and the magnet is allowed to fall with speed  $v$  along the hollow tube. The expression for the induced emf in the coil due to the passing magnet traveling at speed  $v$  using Eq. (2) is

$$\mathcal{E} = N2\pi av B_\rho(a, z) = N2\pi av \frac{3\tilde{\mu}\alpha za}{[a^2 + (\alpha z)^2]^{5/2}}, \quad (A1)$$

where  $z = vt$ . Equation (A1) converts the time interval  $\Delta t$  read along the baseline of the oscilloscope into a distance  $\Delta z$ . The parameter  $\alpha$  is obtained by noting in Eq. (A1) that the coordinate value  $z_m$  corresponding to the maximum  $\mathcal{E}_{\max}$  of the stored transient emf,  $\mathcal{E}(t)$ , occurs for  $\alpha = a/(2z_m)$ . This experiment can be easily repeated and gives a precise value of the parameter  $\alpha$ .

Using Eq. (A1) we write  $B_{\rho, \max} = \mathcal{E}_{\max}/(Nv2\pi a)$ , and in this way,  $B_{\rho, \max}$  may be found from the maximum value,  $\mathcal{E}_{\max}$ , of the stored transient signal. As seen following Eq. (A2), the maximum  $B_{\rho, \max}$  of the radial component of the magnetic field occurs for  $\alpha z = a/2$  and is independent of the value of  $\alpha$ ,

$$B_{\rho, \max} = \frac{3\tilde{\mu}(a/2)a}{[a^2 + (a/2)^2]^{5/2}} = \frac{48\tilde{\mu}}{25\sqrt{5}a^3}, \quad (A2)$$

from which we can obtain  $\tilde{\mu}$ . The two zero crossings of the two transient signals generated by the two pick-up coils are used to find the speed  $v$  of the magnet.

As an example, in one of our experiments, we obtained  $\mathcal{E}_{\max} = 70.0$  mV and  $\Delta t_m = 5.7$  ms  $\pm$  0.2 ms, and for  $a = 10.4$  mm,  $N = 40$ , and  $v = 0.732$  m/s, we obtained  $z_m = 42 \pm 0.2$  mm,  $B_{\rho, \max} = 0.036$  T,  $\alpha = 1.25 \pm 0.05$ , and  $\tilde{\mu} = 4.8 \times 10^{-8}$  Tm<sup>3</sup>. The errors in  $\Delta t_m$  and  $\alpha$  are  $\approx 4\%$ , the experimental errors of the other values are smaller.

<sup>a)</sup>Electronic mail: elladerna@usb.ve

<sup>b)</sup>Electronic mail: pmartin@usb.ve

<sup>1</sup>G. Donoso, C. L. Ladera, and P. Martín, "Magnet fall inside a conductive pipe: Motion and the role of the pipe wall thickness," *Eur. J. Phys.* **30**, 855–869 (2009).

<sup>2</sup>C. S. MacLachy, P. Backman, and L. Bogan, "A quantitative magnetic braking experiment," *Am. J. Phys.* **61**, 1096–1106 (1993).

<sup>3</sup>G. Ireson and J. Twidle, "Magnetic braking revisited: Activities for the undergraduate laboratory," *Eur. J. Phys.* **29**, 745–751 (2008).



- <sup>4</sup>K. D. Hahn, E. M. Johnson, A. Brokken, and S. Baldwin, "Eddy current damping of a magnet moving through a pipe," *Am. J. Phys.* **66**, 1066–1076 (1998).
- <sup>5</sup>M. H. Partovi and E. J. Morris, "Electrodynamics of a magnet moving through a conducting pipe," *Can. J. Phys.* **84**, 253–271 (2006).
- <sup>6</sup>M. A. Heald, "Magnetic braking: Improved theory," *Am. J. Phys.* **56**, 521–522 (1988).
- <sup>7</sup>Y. Levin, S. L. Da Silveira, and F. B. Rizzato, "Electromagnetic braking: A simple quantitative model," *Am. J. Phys.* **74**, 815–817 (2006).
- <sup>8</sup>H. D. Wiederick, N. Gauthier, D. A. Campbell, and P. Rochon, "Magnetic braking: Simple theory and experiment," *Am. J. Phys.* **55**, 500–503 (1987).
- <sup>9</sup>R. Stanway, "Smart fluids: Current and future developments," *Mater. Sci. Technol.* **20**, 931–939 (2004).
- <sup>10</sup>M. R. Jolly, J. W. Bender, and D. J. Carlson, "Properties and applications of commercial magnetorheological fluids," *J. Intell. Mater. Syst. Struct.* **10**, 5–13 (1999).
- <sup>11</sup>D. Halliday, R. Resnick, and K. S. Krane, *Physics*, 4th ed. (Wiley, New York, 1992), Vol. 2, Chap. 36.
- <sup>12</sup>W. M. Saslow, "Maxwell's theory of eddy currents in thin conducting sheets, and applications to electromagnetic shielding and MAGLEV," *Am. J. Phys.* **60**, 693–711 (1992).
- <sup>13</sup>L. H. Cadwell, "Magnetic damping: Analysis of an eddy current brake using an airtrack," *Am. J. Phys.* **64**, 917–923 (1996).
- <sup>14</sup>J. Iñiguez, V. Raposo, A. G. Flores, M. Zazo, and A. Hernández-López, "Magnetic levitation by induced eddy currents in non-magnetic conductors and conductivity measurements," *Eur. J. Phys.* **26**, 951–957 (2005).
- <sup>15</sup>Y. Kraftmakher, "Maglev for students," *Eur. J. Phys.* **29**, 663–669 (2008).
- <sup>16</sup>R. K. Wangsness, *Electromagnetic Fields* (Wiley, New York, 1981), p. 341.
- <sup>17</sup>E. M. Purcell, *Electricity and Magnetism* (McGraw-Hill, New York, 1965), pp. 238–242.
- <sup>18</sup>J. D. Jackson, *Classical Electrodynamics*, 2nd ed. (Wiley, New York, 1975), pp. 177–180.
- <sup>19</sup>Our approximation formula [Eq. (6)] was presented in Ref. 1 and was tested and compared against the circular current loop approximation found in Ref. 18, and it represents the measured experimental values of the magnet magnetic field with good accuracy. This approximation considers the nonzero second-order term in the expansion of the magnetic moment in terms of Legendre polynomials [Ref. 1, Eq. (28)].

The *American Journal of Physics* invites you to submit papers for a special theme issue **Using Astronomy and Space Science Research in Physics Courses**.

Decades of research in physics, astronomy, and space science have led to remarkable new instruments and technologies and astonishing discoveries. With this theme issue we propose to harvest some of this abundance to enliven and update physics instruction.

We wish to publish papers that describe achievements of astronomy and space science research and highlight their underlying physics and lay out realistic ways to use this material for physics instruction.

Our invitation is a challenge

- to astronomers, space scientists, and physicists to describe discoveries and technologies and to emphasize their physics content in ways that will help physicists use them in their teaching;
- to teachers of physics and astronomy to develop or renew curricula by infusing them with discoveries and technologies of astronomy and space science;
- to astronomy and physics education researchers to
  - identify the basic concepts needed for students to understand the discoveries and technologies of astronomy and space science,
  - explore how the discoveries and technologies can be presented to most effectively realize the goals of physics instruction,
  - provide tools to assess how well students achieve the goals.

This theme issue will be published in spring 2012. **The deadline for submission of articles is September 15, 2011.** Please submit papers for the theme issue to *AJP* in the usual way, but indicate your interest in submitting to the theme issue. To ask questions or make suggestions about the theme issue, contact the guest editors Peter Shaffer (shaffer@phys.washington.edu) or Charles H. Holbrow (cholbrow@mit.edu).

**Using Astronomy and Space Science Research in Physics Education** will be the topic of the next Gordon Research Conference on Physics Research and Education to be held in June 2012. The exact date and location are still to be determined. The co-chairs are Peter Shaffer, University of Washington, and Charles H. Holbrow, Colgate University; the vice chairs are Matthew Lang, Massachusetts Institute of Technology, and Mel Sabella, Chicago State University.